
Original Paper

Performance Enhancement of 20kW Regenerative Blower Using Design Parameters

Choon-Man Jang¹ and Hyun-Jun Jeon¹

¹Environmental Engineering Research Division, Korea Institute of Construction Technology
283 Goyangdae-Ro, Ilsanseo-Gu, Goyang, Gyeonggi-Do, 411-712, Republic of Korea,
jangcm@kict.re.kr, jeonhj@kict.re.kr

Abstract

This paper describes performance enhancement of a regenerative blower used for a 20 kW fuel cell system. Two design variables, bending angle of an impeller and blade thickness of an impeller tip, which are used to define an impeller shape, are introduced to enhance the blower performance. Internal flow of the regenerative blower has been analyzed with three-dimensional Navier-Stokes equations to obtain the blower performance. General analysis code, CFX, is introduced in the present work. SST turbulence model is employed to estimate the eddy viscosity. Throughout the numerical analysis, it is found that the thickness of impeller tip is effective to increase the blower efficiency in the present blower. Pressure is successfully increased up to 2.8% compared to the reference blower at the design flow condition. And efficiency is also enhanced up to 2.98 % compared to the reference one. It is noted that low velocity region disturbs to make strong recirculation flow inside the blade passages, thus increases local pressure loss. Detailed flow field inside the regenerative blower is also analyzed and compared.

Keywords: Regenerative Blower, Design Parameter, Pressure, Blower Efficiency, Numerical Simulation.

1. Introduction

Internal flow analysis using two design parameters of a regenerative blower used for a 20 kW fuel cell system has been performed to enhance the performance of the blower in the present study. A regenerative blower is widely used in the industrial fields: flow circulator of waste water in a sewage disposal tank, BOP of a fuel cell system, core part of medical equipment, and so on. The blower needs high pressure and constant flow rates. According to the shapes of a blower impeller, the blower has two types of impellers: the open and side channel type. Open channel type impeller is widely selected in the industrial fields due to relatively lower manufacturing costs. Design of a high efficient blower is very important to get higher exit pressure.

Optimal shape design of a regenerative blower using some design parameters is recently introduced to enhance the performance of a regenerative blower. [1-3] Characteristic of design parameters was reported by researchers. [1,3] They showed that optimal shape design on an impeller and a casing could increase the performance of the blowers.

Recently optimal design method using response surface method (RSM) [4,5] combined with three-dimensional Navier-Stokes solver is used to find optimum shapes of a blower. The RSM is global optimization and can find easily optimal position using the results. The method also can utilize information collected from various sources, thus effective for both of single- and multi-disciplinary optimization problems [6]. In the previous study, Jang and Han [2] tried to optimize the shape of impeller for two stage ring blower. Also, Jang and Lee[7] tried to make the shape optimization of a regenerative blower used for building fuel cell system by RSM combined with numerical simulation.

In the present study, a numerical investigation on the aerodynamic performance of a regenerative blower has been carried out based on three-dimensional Reynolds-averaged Navier-Stokes (RANS) equations. A parametric study is carried out with two design variables: bending angle of impeller and blade thickness of an impeller tip. Pressure and efficiency of the blower are selected as an objective function for the present study. Detailed internal flow analysis is also performed and compared with the reference blower.

2. Reference Regenerative Blower

A regenerative blower used for a 20 kW fuel cell system is introduced in the present study. The detailed specifications of the blower are summarized in Table 1. The inlet and outlet duct diameter of the impeller used in the present study is 51 mm. The perspective view of the test blower is shown in Fig. 1. The blower consists of a casing and an impeller. As shown in the Fig.1, impeller blade has an open channel type, and the number of an impeller blade is 54.

Fig. 2 shows performance curve of tested regenerative blower obtained by numerical simulation, maximum efficiency is observed ner the design flow condition.

Table 1 Design specifications for the regenerative blower

Design Flow rate, lpm	2,000	Outlet diameter of impeller, mm	256.3
Rotational frequency of impeller, r/min	3300	Inlet diameter of impeller, mm	185
Efficiency, %	44	Number of main blades	54

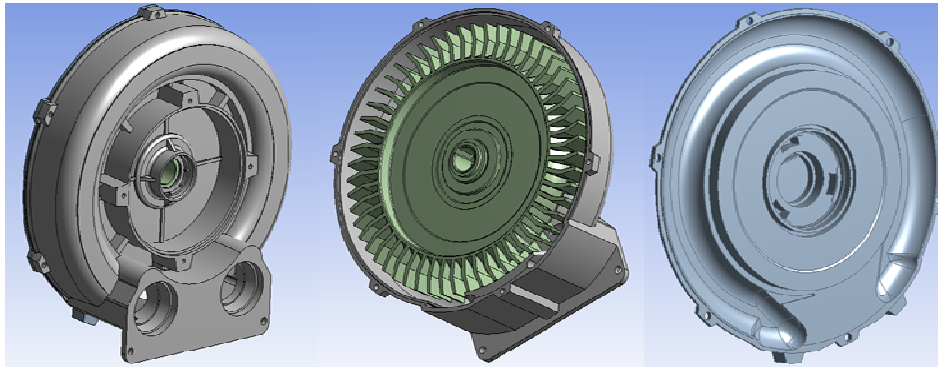


Fig. 1 Configuration of tested regenerative blower

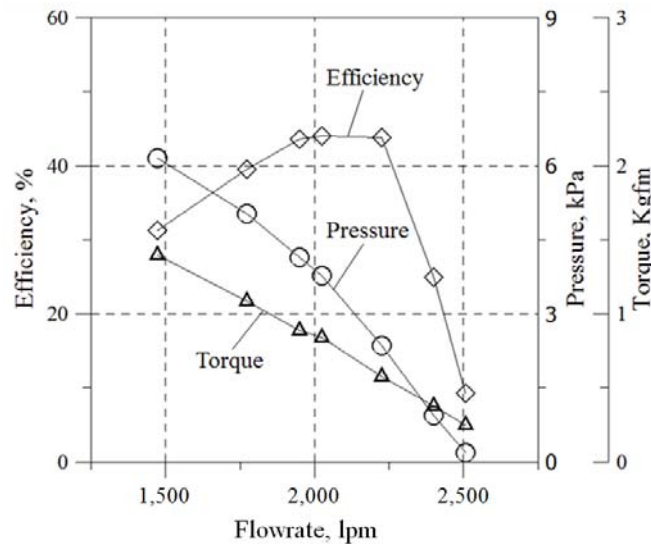


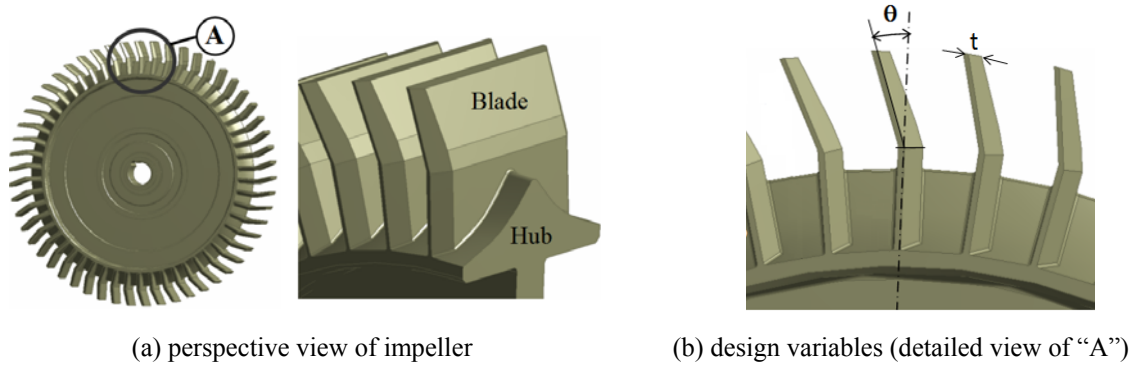
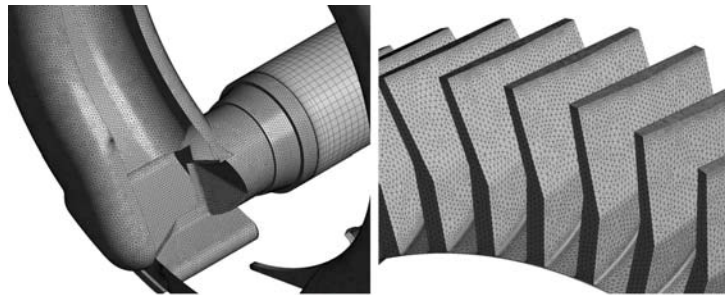
Fig. 2 Performance curve

3. Definition of Design Parameters

In the present study, pressure and efficiency are selected as target value (object function) to the blower. To enhance the performance of the blower, the shape of the blower impeller is optimized by introducing two design variables: bending angle of an impeller (θ) and blade thickness of an impeller tip (t) as shown in Fig. 3, similarly to previous study [2]. The bending angle of an impeller and blade thickness of an impeller tip for the reference blower is 18° and 3 mm, respectively. The range of the design parameters is determined by preliminary calculation, and listed in Table 2.

Table 2 Design Variables

Variables	Lower Bound	Middle	Upper Bound
θ , Bending angle of impeller blade	14°	18°	22°
t, Thickness of impeller blade tip	1mm	2mm	3mm

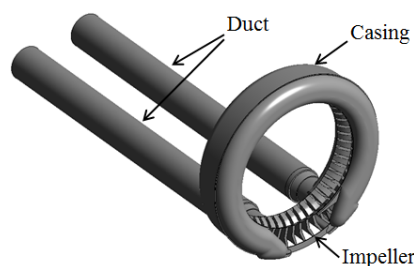
**Fig. 3** Definition of design Variables (θ , t) [2]**Fig. 4** Computational grid

4. Numerical Simulation

To determine the performance of the blower and analyze the flow characteristics inside the blower, general analysis code, CFX-13 [8], is introduced in the present study. It solves compressible Reynolds-averaged Navier-Stokes equations (RANS) and a continuity equation. SST turbulence model with scalable wall function is employed to estimate the eddy viscosity [9]. In computational grids, unstructured grids are used to represent a composite grid system including the impeller and casing domains.

Fig. 4 shows the computational grid system. Tetrahedral element is mainly imposed in the casing and impeller where wedge (prism) element having three layers is introduced near the wall. Hexahedral element is also imposed in the inlet and outlet duct to reduce the grid nodes. The whole grid system in the present simulation has about 3,650,000 nodes.

As boundary conditions, atmospheric pressure is specified at the inlet, and mass flow rate is specified at the exit. No-slip and adiabatic wall conditions are used on impeller blade and casing surfaces. Boundary plane between the impeller and casing regions is imposed frozen rotor interference. Fig. 5 shows separated region for numerical simulation, which has ducts, a blower impeller and casing. The length of ducts is chosen with 10 times of duct diameter.

**Fig. 5** Separated region for numerical simulation

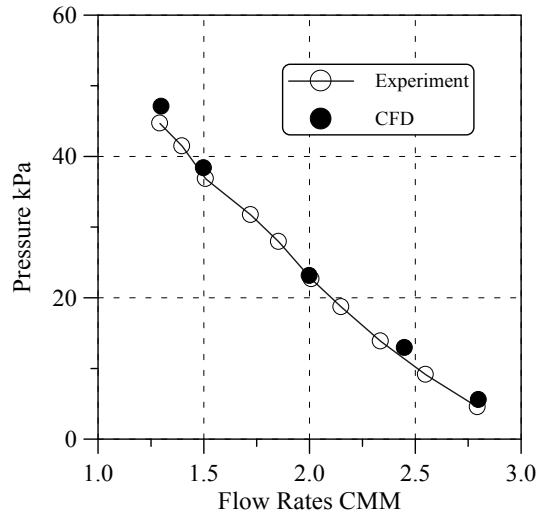


Fig. 6 Comparisons of blower performance [2]

5. Validation of Numerical Simulation

In the previous study, authors [2] tried to optimize the shape of impeller for two-stage regenerative blower by RSM combined with numerical simulation. For the validation of the numerical solutions, the pressure rise for the reference blade was compared to the experimental results according to flow rates in Fig. 6. The figure shows that the distributions of local pressure obtained by numerical simulation match well with the experimental results for the reference shape. The computed pressure, object function in the blade optimization, has a maximum of 5 percent error with the experimental data. The comparisons between the numerical and experimental results show that the pressure of the regenerative blower is simulated correctly.

6. Results and Discussion

To analyze the performance of the regenerative blower having a different design condition, internal flow is compared using the results of numerical simulation.

Fig. 7 shows the distributions of streamlines colored with velocity for the reference blower, which is side view from the impeller. The flow come through the inlet duct is separated to the both sides of the impeller in the casing inlet region. Relatively higher velocity is observed in the right side because of short moving length from the inlet duct. Strong radial flow is observed at the middle of blade passage due to centrifugal force, which results in the pressure increase at each blade passage.

Fig. 8 shows the tangential velocity vectors on the three orthogonal planes to the rotational direction for the reference blower. The positions of each plane represent in Fig. 8(a). Non-symmetric recirculation flow is formed in the blade passage at the inlet and outlet region (Plane 1, 3) while symmetric recirculation flow is formed at the middle blade passage (Plane 2). Non-symmetric recirculation flow generated near the inlet and outlet region of the impeller is mainly caused by the distorted flow inside blade passage. On the Plane 1, relatively strong recirculation is found on the right hand side. In the same manner, on the plane 3, relatively strong recirculation is found on the left hand side.

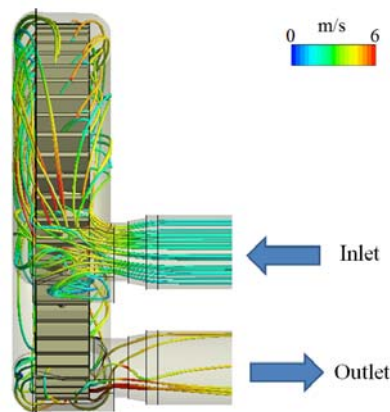


Fig. 7 Streamlines colored with velocity for reference blower

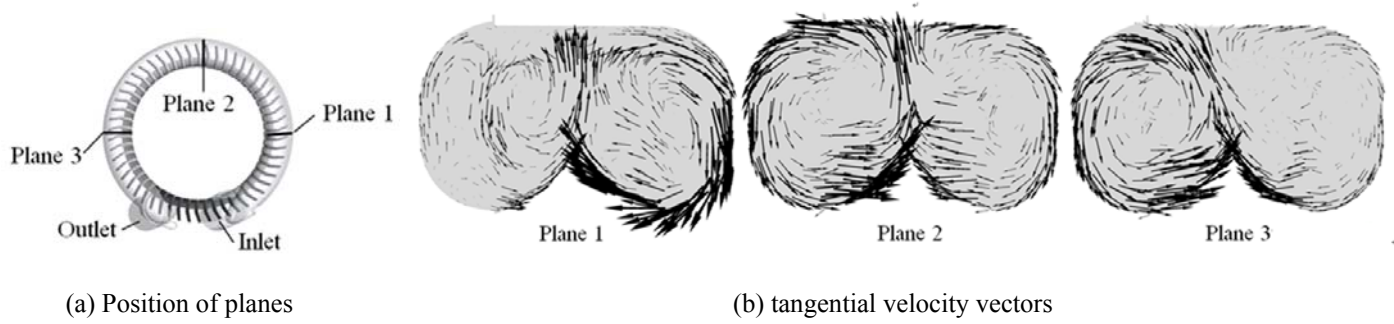


Fig. 8 Tangential velocity vectors for reference blower

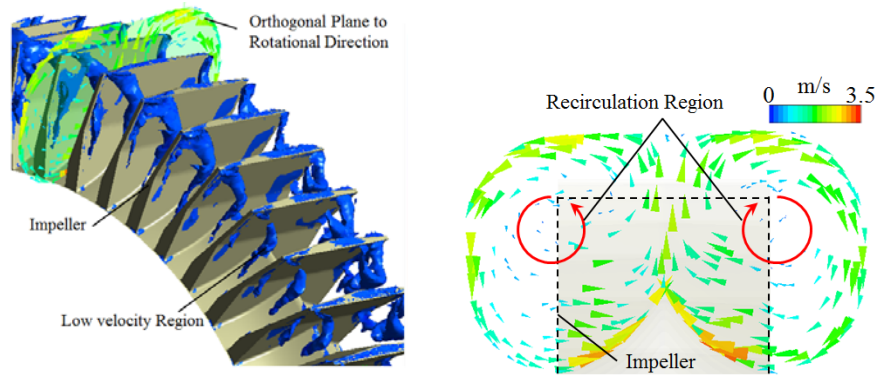


Fig. 9 Iso-surface having low velocity of 5 m/s ($t=1\text{mm}$)

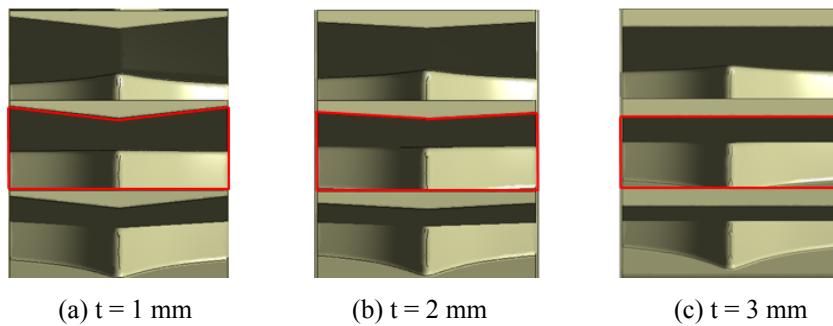


Fig. 10 Top view of blade passage for different blade tip thickness

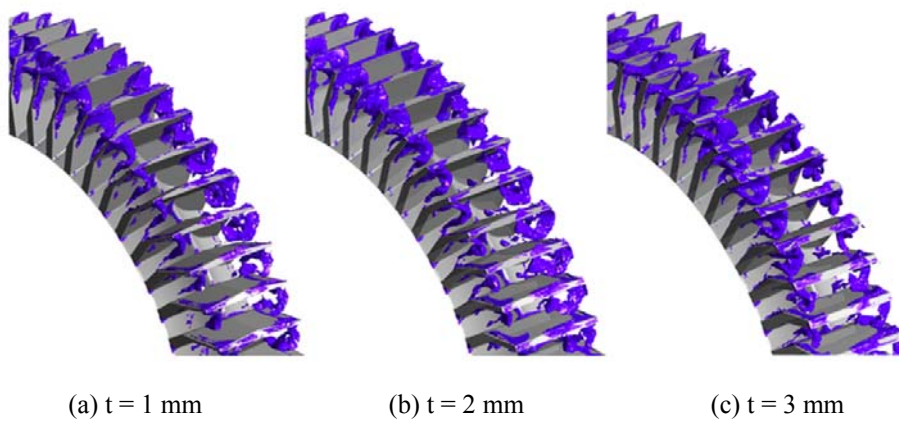


Fig. 11 Iso-surface having low velocity of 5 m/s ($\theta = 22\text{deg}$).

Fig. 9 shows the distributions of iso-surfaces having a low velocity of 5 m/s. In the figure, the low velocity region is formed in the both sides of the impeller. The low velocity region is formed near the center position of a recirculation flow. The low velocity region is induced by horizontal inlet flow and outlet flow having a radial component as shown in Fig. 9.

Fig. 10 shows the top view of blade passage for different blade tip thickness. As shown in the figure, blade passage increases as the blade thickness decreases.

Fig. 11 shows the distributions of an iso-surface having the low velocity of 5 m/s for $\theta = 22$ degree. In the figure, the low velocity region is formed in both sides of the impeller. In the figure, low velocity region is expanded according to the increase of the impeller tip thickness because recirculation region is decreased due to viscous effect caused by the deduced blade passage shown in Fig. 10. From the flow analysis, it is known that the reduction of low velocity region formed in the both sides of the impeller is necessary to increase the performance of the blower.

Fig. 12 shows the pressure distributions for the different design conditions. The measuring position is along the casing wall from inlet to outlet as shown in Fig. 12(a). Linear increase of pressure is observed for all cases along the measuring positions. It is noted that the pressure increase is caused by momentum force generated inside blade passage. The momentum force is due to the recirculation flow observed in Fig. 7. As shown in the figure, relatively higher pressure is observed at $t = 1$ mm. Pressure is successfully increased up to 2.8% compared to the reference blower at the design flow condition. As mentioned above through Fig. 9-11, it is noted that the more thickness of impeller tip is thin, the stronger recirculation flow is generated.

Fig.13 shows blower efficiency according to the variations of design variables. The blower efficiency is determined by using the pressure at the outlet of the duct. As shown in the figure, blower efficiency has a maximum value at the impeller thickness of 2 mm while impeller bending angle is 14 degree. From the Fig. 10, blower efficiency can be increase up to 2.98% compared to the reference blower at the design flow condition.

Fig.14 shows the velocity contours at the blower outlet according to the bending angle of an impeller and the blade thickness of an impeller tip. The position of the blower outlet is in Fig. 14(a). As shown in the figure, relatively larger velocity distortion is observed at the impeller tip thickness of 1mm for impeller bending angles compared to that of 2 and 3 mm.

Fig. 15 shows the velocity vectors colored by velocity at the blower outlet according to the blade thickness of an impeller tip for $\theta=14^\circ$. As shown in the figure, relatively high secondary flow is observed at $t=1$ mm (“A” in Fig. 15), which disturbs pressure increase in the blower. Due to the non-uniform flow at the blower outlet, pressure increase can be deteriorated by velocity defect. Relatively uniform blower outlet flow is observed at the impeller thickness of 2 mm and impeller bending angle of 14 degree where the blower efficiency has maximum value.

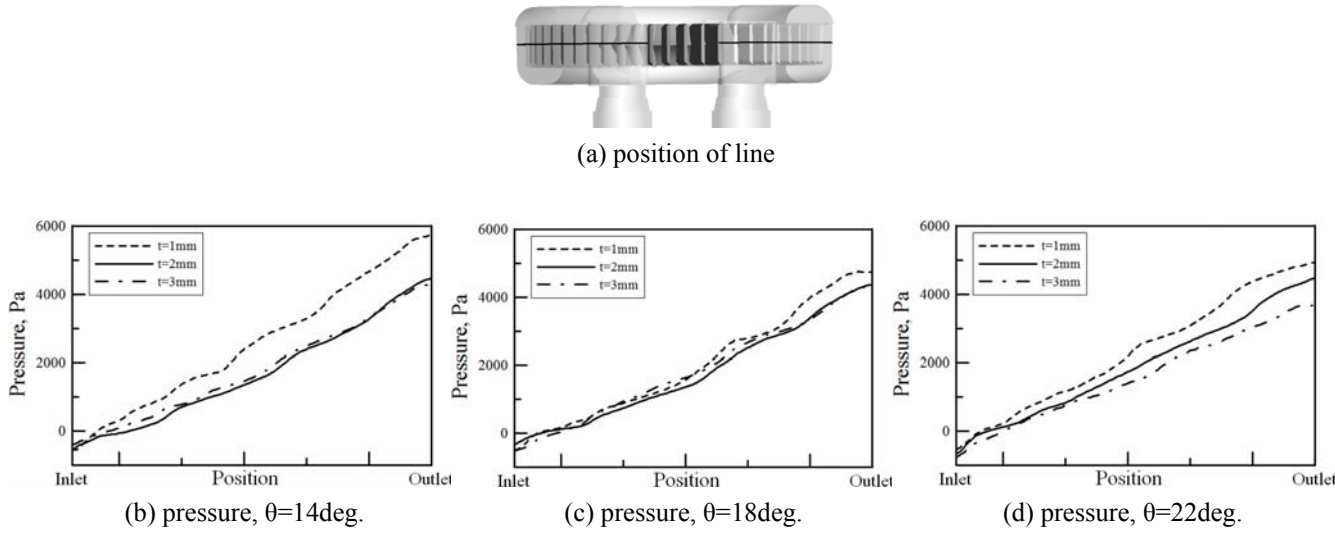


Fig. 12 Pressure distributions along the casing wall

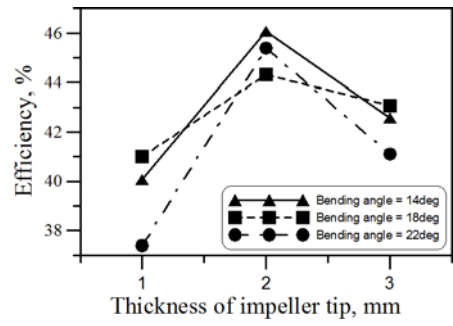


Fig. 13 Blower efficiency according to design variables

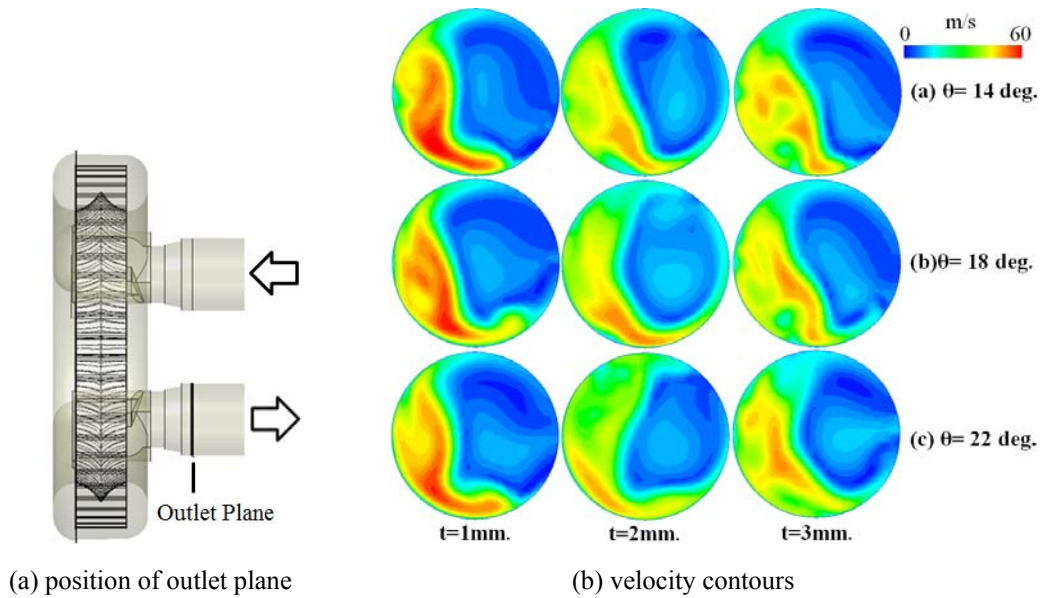


Fig. 14 Velocity contours at the blower outlet

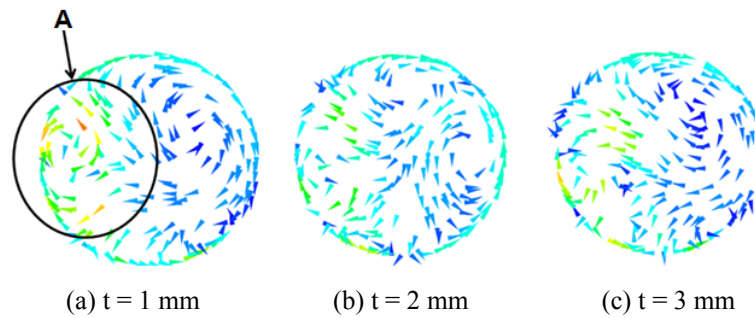


Fig. 15 Velocity vector at the blower outlet (For $\theta=14^\circ$)

7. Conclusion.

Performance of a regenerative blower used for a 20 kW fuel cell system has been analyzed by numerical simulation. Two design variables, bending angle of an impeller and blade thickness of an impeller tip, are introduced to enhance the pressure and efficiency at the design flow condition.

From the internal flow analysis, the low velocity region due to recirculation flow is formed at the center of recirculation flow inside blade passages. Low velocity region disturbs to make strong recirculation flow inside each blade passage, thus results in local pressure loss at each blade passage. It is noted that the pressure increase is caused by momentum force generated inside the blade passages. Relatively higher pressure is observed at $t = 1\text{mm}$ compared to that of $t = 2$ and 3mm .

Throughout the analysis of the design variables in the regenerative blower, pressure is successfully increased up to 2.8 % compared to the reference blower at the design flow rate. And efficiency is also increased up to 2.98 % compared to reference one. Relatively uniform blower outlet flow is observed at maximum efficiency condition of the blower. It is well known that non-uniform flow at the blower outlet increases pressure loss by velocity defect.

Acknowledgments

This study was supported by the major project (2014-0085) of the Korea Institute of Construction Technology.

References

- [1] Jang, C.-M., Lee, J.-S., Tak, B.-Y. and Kim, C.-G., "Characteristics of Design Parameters for an Industrial Regenerative Blower," *Proceedings of the Summer Conference of The Society of Air-Conditioning and Refrigerating Engineers of Korea*, Yongpyeong Resort, June 2012, pp. 175-178. (in Korean)
- [2] Jang, C.-M. and Han, G.-Y., 2010, "Enhancement of Performance by Blade Optimization in Two-Stage Ring Blower," *J Thermal Science*. Vol. 19, No. 5, pp. 383-389.
- [3] Choi, Y.-S., Lee, K.-Y., Jeong, K.-H., Kim, Y.-K. and Seo, J.-M., 2011, "Design and Performance Evaluation of Side Channel Type Regenerative Blower," *KSME Manufacturing and Design Engineering Division Spring Conference*. (in Korean)
- [4] Myers, R. H., and Montgomery, D. C., 1995, "Response Surface Methodology: Process and Product Optimization Using Designed Experiments," *John Wiley & Sons, New York*.
- [5] Kim, J.-H. and Kim, K.-Y., 2011, "Optimization of Vane Diffuser in a Mixed-Flow Pump for High Efficiency Design," *International Journal of Fluid Machinery and System*, Vol. 4, No. 1, pp. 172-178.
- [6] Sevant, N. E., Bloor, M. I. G., and Wilson, M. J., 2000 "Aerodynamic Design of a Flying Wing Using Response Surface Methodology," *J. Aircraft*, Vol. 37, pp. 562-569.
- [7] Jang, C.-M., Lee, J.-S., "Shape optimization of a regenerative blower used for building fuel cell system." *Proceedings of 4th Asian Joint Workshop on the Thermophysics and Fluid Science*, Busan, Oct 2012. (in Korean)
- [8] CFX-13 User Manual, Ansys inc., 2011.
- [9] Menter, F. R., 1994, "Two-Equation Eddy-Viscosity Turbulence Models for Engineering Application," *AIAA Journal*, Vol. 32, No. 8, pp. 1598-1605.